HYDRODYNAMIC MODELLING AND OPTIMAL CONTROL OF TIDAL POWER SCHEMES IN LONG ESTUARIES

Z.G.Xu and N.K.Nichols

Numerical Analysis Report 6/91

Department of Mathematics
University of Reading
Whiteknights, P.O.Box 220
Reading RG6 2AX

The work reported here has been funded by National Power PLC and forms part of the research programme of the Reading/Oxford Institute for Computational Fluid Dynamics.

Abstract

Non-linear optimal control problems in tidal power generation are formulated and thoroughly investigated. The formulation is based on a dynamic flow model in which the fluid dynamics in the full estuary and across a tidal barrage are described by the time-dependent non-linear shallow water equations. By using the Lagrangian method, necessary conditions for control optimality are derived. To obtain the precise form of the solution for the problem, a numerical solution procedure is adopted. It consists of a constrained optimisation algorithm for iteratively determining optimal sluice and turbine control functions, together with a finite difference scheme for solving the flow and adjoint equations. The emphasis of the numerical work is placed on the optimisation algorithm. Several gradient based optimisation algorithms are presented and the behaviours of the algorithms are examined in detail. Both ebb only generation and two-way generation results are given.

Contents

List of Figures

List of Tables

1 Introduction

In [1] we reported detailed results of our investigation of optimal control problems for tidal power schemes with sluices and turbines operating independently. Analytically it was deduced from Pontryagin's Maximum Principle that the optimal sluice control function is invariably bang-bang in nature; whereas the optimal turbine control function is dependent on the form of the power function. For a linear power function, a bang-bang solution results. For a non-linear power function, the solution is no longer bang-bang but contains some interior points. These conclusions were confirmed by extensive and systematic numerical work which utilised several gradient based optimisation algorithms. The equation governing the flow across the barrage was solved by a finite difference method using the trapezoidal scheme. Upon examination of the performance of the algorithms, it was concluded that the conditional gradient algorithm was best suited for bang-bang type controls, while for the type of controls with interior points the projected gradient algorithm was recommended. Similar work was also reported in [2] but with only one control.

The formulation in [1] and [2] was based on a flat basin flow model which assumes that the basin surface elevation remains flat everywhere throughout the basin and that the flow across the barrage is governed by an ordinary differential equation. The main advantage of this model is that it is simple to use. However it takes no account of the different phases of the tides at different points along the estuary. As a result it cannot be expected to give an accurate estimate of power output from a tidal scheme and hence its application can be severely restricted. More accurate estimates can only be achieved by employing more sophisticated and more accurate flow models which are capable of accounting for the dynamic effects in the basin. Mathematically the flow is treated as a function of both time and spatial position, and the system is described by a set of partial differential equations.

In this report the optimal control problem for a tidal power scheme based on a dynamic model (also known as the partial differential equation model) is investigated. Firstly the flow equations governing the fluid dynamics in an estuary and across the tidal barrage are described, together with the associated initial and boundary conditions. Then the optimal control problem is formulated and the necessary conditions for optimality are derived. A detailed description of the numerical solution procedure, in particular, the finite difference scheme, is given thereafter. Finally numerical results for the Severn estuary tidal barrage scheme are presented.

2 The Mathematical Model

2.1 The Equations of Flow

The basic geometry of the estuary together with a tidal barrage is given in Fig.1. It shows that the tidal basin lies upstream of the tidal barrage which is itself situated at $x = 0$. If the estuaries of interest are long compared to their width, then the flow can be treated as one-dimensional within reasonable accuracy. As a result the fluid dynamics in the estuary can be modelled by the time-dependent one-dimensional shallow water equations, which are

Continuity equation:

$$b(\eta, x)\frac{\partial \eta}{\partial t} + \frac{\partial (A(\eta, x)u)}{\partial x} = 0 \tag{1}$$

Momentum equation:

$$\frac{\partial u}{\partial t} + u\frac{\partial u}{\partial x} + g\frac{\partial \eta}{\partial x} + \frac{gn^2 u|u|}{r^{4/3}(\eta, x)} = 0 \tag{2}$$

where

$\eta(x, t)$ = water surface elevation above datum,
$u(x, t)$ = velocity in x - coordinate direction,
g = acceleration due to gravity,
n = Manning's constant,
$b(\eta, x)$ = breadth,
$A(\eta, x)$= vertical cross-sectional area,
$r(\eta, x)$ = hydraulic radius of the channel. For a wide shallow estuary, r can be approximated by the formula $r(\eta, x) = A(\eta, x)/b(\eta, x)$.

There are two types of boundary conditions with this problem: external and internal. The external boundary conditions are chosen to give no flow through the upstream boundary at $x = l_2$, and to give a specified variation with time of water level at $x = -l_1$ which is the mouth of the estuary. Hence we have

$$\eta(-l_1, t) = f(t) \quad , \quad u(l_2, t) = 0 \tag{3}$$

where $f(t)$ = tidal elevation. Over a short interval of time the tides are approximately periodic, hence $f(t) = f(t + T)$, where T is the tidal period. It follows therefore that the water surface elevation $\eta(x, t)$ and the velocity $u(x, t)$ must also be periodic in time with period T. Hence the following periodicity conditions are evident

$$\eta(x, 0) = \eta(x, T) \quad , \quad u(x, 0) = u(x, T) \tag{4}$$

In addition to these external boundary and periodicity conditions, there exists an internal boundary condition due to the presence of the tidal barrage in the flow path. This can be expressed by the mass continuity requirement across the barrage

$$Q(0,t) = A(\eta^+, 0^+)u(0^+, t) = A(\eta^-, 0^-)u(0^-, t) \tag{5}$$

where $Q(0,t)$ is the total volumetric flow rate of water across the barrage at any time t. On the other hand, it is also the total volumetric flow rate of water through sluices and turbines. Hence it can be given alternatively by

$$Q(0,t) = \alpha_S(t)X_S(h) + \alpha_T(t)X_T(h) \tag{6}$$

where

$h = \eta(0^-, t) - \eta(0^+, t)$ is the head difference across the tidal barrage,

$\alpha_S(t)$ and $\alpha_T(t)$ are the sluice control function and the turbine control function respectively. The control functions represent the percentage of the maximum total flow which is permitted through each device at a particular time t and are bounded such that

$$0 \le \alpha_S(t) \le 1 \tag{7}$$

$$0 \le \alpha_T(t) \le 1. \tag{8}$$

The functions X_S, X_T are used to denote the maximum total fluxes permitted through sluices and turbines respectively. These are further defined as

$$X_S(h) = \begin{cases} -Q_{S1}(h) & \text{if } h \le 0 \\ Q_{S2}(h) & \text{otherwise} \end{cases} \tag{9}$$

$$X_T(h) = \begin{cases} -Q_{T1}(h) & \text{if } h \le 0 \\ Q_{T2}(h) & \text{otherwise} \end{cases} \tag{10}$$

where

$Q_{S1}(h)$ is the maximum sluice flow out of the basin for head h,
$Q_{S2}(h)$ is the maximum sluice flow into the basin for head h,
$Q_{T1}(h)$ is the maximum turbine flow out of the basin for head h,
$Q_{T2}(h)$ is the maximum turbine flow into the basin for head h.

2.2 The Optimal Control Problem

Having set up the equations governing the flow in the estuary and across the barrage, we can formulate the optimal control problem for a tidal power generation scheme with two controls as follows: we seek to determine a control vector $\underline{\alpha}=(\alpha_S, \alpha_T)^T$ which maximises the power functional

$$E = \int_o^T e(X_T(h)\alpha_T, h)dt \tag{11}$$

subject to the constraints expressed by Eqns.(1)-(8).

The integrand in Eqn.(11) is the instantaneous power function of turbine flow and head difference across the barrage.

2.3 Necessary Condition for Optimality

In this section we derive necessary conditions for optimality for the problem under consideration. Pontryagin's Maximum Principle has been used successfully in [1] [2] where the flow is described by an ordinary differential equation. However, with a system of partial differential equations the Maximum Principle is no longer directly applicable. To solve problems of this form, we must resort to the more general Lagrangian method.

The Lagrangian functional associated with this optimal control problem can be constructed as (Ref.[5]):

$$L(\underline{\alpha}) = \int_0^T \Big[e(X_T(h)\alpha_T, h) + \gamma_1[A(\eta_o^-, 0^-)u_o^- - \alpha_S X_S(h) - \alpha_T X_T(h)] + \gamma_2[A(\eta_o^-, 0^-)u_o^- - A(\eta_o^+, 0^+)u_o^+]\Big]\, dt +$$

$$\int\!\!\!\!-_{-l_1}^{l_2} \int_0^T \left[\lambda\left(-\frac{\partial A}{\partial t} - \frac{\partial Q}{\partial x}\right) + \mu\left(-\frac{\partial u}{\partial t} - u\frac{\partial u}{\partial x} - g\frac{\partial \eta}{\partial x} - gn^2 u|u|\frac{1}{r^{4/3}}\right)\right] dx dt \qquad (12)$$

where $Q = Au$, $u_o^\pm = u(0\pm, t)$, $\eta_o^\pm = \eta(0\pm, t)$ and the functions $\gamma_1(t)$, $\gamma_2(t)$, $\lambda(x,t)$, $\mu(x,t)$ are Lagrangian multipliers, and

$$\int\!\!\!\!-_{-l_1}^{l_2} f(x)dx = \int_{-l_1}^{0^-} f(x)dx + \int_{0+}^{l_2} f(x)dx \qquad (13)$$

The total variation of the Lagrangian is given by

$$\triangle L = \delta L + \frac{1}{2}\delta^2 L + \cdots \qquad (14)$$

where δL and $\delta^2 L$ denote the first and second variation of the Lagrangian. We shall only derive the first variation as it sets out the necessary condition for optimality. If we take a weak variation in $\underline{\alpha}$ and make use of integration by parts, then we can write the first variation in the following form

$$\begin{aligned}\delta L(\underline{\alpha}, \delta\underline{\alpha}) \;=\; & \int_0^T \Big[\frac{\partial e}{\partial \alpha_T}\delta\alpha_T + \frac{\partial e}{\partial h}\delta h + \gamma_1[\delta Q_0 - (\alpha_S X_S' + \alpha_T X_T')\delta h - X_S\delta\alpha_S - X_T\delta\alpha_T] \\ & \gamma_2(b_o^- u_o^- \delta\eta_o^- + A_o^-\delta u_o^- - b_o^+ u_o^+ \delta\eta_o^+ - A_o^+\delta u_o^+)\Big]\, dt \\ & + \int_0^T \Big[(-\lambda\delta Q - \mu u\delta u - g\mu\delta\eta)|_{-l_1}^{0^-} + (-\lambda\delta Q - \mu u\delta u - g\mu\delta\eta)|_{0+}^{l_2}\Big]\, dt + \\ & \int\!\!\!\!-_{-l_1}^{l_2} (-\lambda\delta A - \mu\delta u)|_0^T dx + \int\!\!\!\!-_{-l_1}^{l_2} \int_0^T \Big[\frac{\partial \lambda}{\partial t}\delta A + \frac{\partial \lambda}{\partial x}\delta Q + \frac{\partial \mu}{\partial t}\delta u + u\frac{\partial \mu}{\partial x}\delta u + g\frac{\partial \mu}{\partial x}\delta\eta\end{aligned}$$

$$- \mu g n^2 \left(2|u| \frac{1}{r^{4/3}} \delta u - \frac{4}{3} u|u| \frac{\partial r}{\partial \eta} \frac{1}{r^{7/3}} \delta \eta \right) \Big] \, dx dt \tag{15}$$

where $Q_o = Q(0,t)$ is the total volumetric flow rate of water across the barrage.

This expression can be rearranged by considering the relations $\delta Q = A\delta u + u\delta A$, $\delta A = b\delta\eta$ and $\delta h = \delta\eta_0^- - \delta\eta_0^+$. Upon making these substitutions and expressing the variations of the dependent variables in terms of $\delta\eta$ and δu, the first variation becomes

$$\begin{aligned}
\delta L(\underline{\alpha}, \delta\underline{\alpha}) = & \int_0^T \left[\left(\frac{\partial e}{\partial \alpha_T} - \gamma_1 X_T \right) \delta\alpha_T + (-\gamma_1 X_S) \delta\alpha_S \right] dt + \\
& \int_0^T \left[\frac{\partial e}{\partial h} \delta h + \gamma_1 [\delta Q_0 - (\alpha_S X_S' + \alpha_T X_T') \delta h] \right] dt + \\
& \int_0^T \left[(-\lambda \delta Q - \mu u \delta u - g \mu \delta\eta)|_{-l_1}^{0^-} + (-\lambda \delta Q - \mu u \delta u - g\mu\delta\eta)|_{0^+}^{l_2} \right] dt + \\
& \int_0^T \gamma_2 (b_o^- u_o^- \delta\eta_o^- + A_o^- \delta u_o^- - b_o^+ u_o^+ \delta\eta_o^+ - A_o^+ \delta u_o^+) dt \\
& \int_{-l_1}^{l_2} [-\lambda \delta A - \mu \delta u]_0^T dx + \int_{-l_1}^{l_2} \int_0^T \left\{ \left[b \left(\frac{\partial \lambda}{\partial t} + u \frac{\partial \lambda}{\partial x} \right) + g \frac{\partial \mu}{\partial x} + \frac{4 \mu g n^2 u|u|}{3 r^{7/3}} \frac{\partial r}{\partial \eta} \right] \delta\eta \right. \\
& \left. + \left[\frac{\partial \mu}{\partial t} + u \frac{\partial \mu}{\partial x} + A \frac{\partial \lambda}{\partial x} - \frac{2 \mu g n^2 |u|}{r^{4/3}} \right] \delta u \right\} dx dt
\end{aligned} \tag{16}$$

The necessary condition for $\underline{\alpha}(t)$ to be optimal is that the first variation $\delta L(\underline{\alpha}, \delta\underline{\alpha})$ of the Lagrangian L must be non-positive. Mathematically this condition can be expressed as

$$\delta L(\underline{\alpha}, \delta\underline{\alpha}) \leq 0 \tag{17}$$

It is observed that the adjoint variables λ and μ can be selected so that the integrands of all the integrals except the first one vanish. This leads to adjoint equations of the form

$$b(\eta, x) \left(\frac{\partial \lambda}{\partial t} + u \frac{\partial \lambda}{\partial x} \right) + g \frac{\partial \mu}{\partial x} + \frac{4 \mu g n^2 u|u|}{3 r^{7/3}} \frac{\partial r}{\partial \eta} = 0 \tag{18}$$

$$\frac{\partial \mu}{\partial t} + u \frac{\partial \mu}{\partial x} + A \frac{\partial \lambda}{\partial x} - \frac{2 \mu g n^2 |u|}{r^{4/3}} = 0 \tag{19}$$

with the external boundary conditions

$$A\lambda + \mu u = 0 \qquad \text{at } x = -l_1 \tag{20}$$

$$\mu = 0 \qquad \text{at } x = +l_2 \tag{21}$$

and the internal boundary conditions

$$\mu(0^+,t)(g - b_o^+(u_o^+)^2/A_o^+) + \gamma_1[\alpha_S X_S(h)' + \alpha_T X_T(h)'] = \frac{\partial e}{\partial h} \tag{22}$$

$$\mu(0^+,t)(g - b_o^+(u_o^+)^2/A_o^+) = \mu(0^-,t)(g - b_o^-(u_o^-)^2/A_o^-) \tag{23}$$

where

$$\gamma_1(t) = \lambda_0^- - \lambda_0^+ + \mu_0^- u_0^-/A_0^- - \mu_0^+ u_0^+/A_0^+ \tag{24}$$

$$\gamma_2(t) = \lambda_0^+ + \mu_0^+ u_0^+/A_0^+ \tag{25}$$

and the periodicity conditions

$$\lambda(x,0) = \lambda(x,T) \tag{26}$$

$$\mu(x,0) = \mu(x,T) \tag{27}$$

where $\lambda_o^\pm = \lambda(0\pm,t)$, $\mu_o^\pm = \mu(0\pm,t)$.

Finally, the necessary condition for optimality can be written as

$$\delta L(\underline{\alpha}, \delta\underline{\alpha}) = \int_0^T \underline{\nabla} E(\underline{\alpha}) \cdot \delta\underline{\alpha} \; dt \le 0 \tag{28}$$

where $\underline{\nabla} E(\underline{\alpha})$ is the functional gradient and can be calculated as follows

$$\underline{\nabla} E(\underline{\alpha}) = \left\{ \begin{array}{c} \partial E/\partial\alpha_T \\ \\ \partial E/\partial\alpha_S \end{array} \right\} = \left\{ \begin{array}{r} \partial e/\partial\alpha_T - \gamma_1(t) X_T(h) \\ \\ -\gamma_1(t) X_S(h) \end{array} \right\} \tag{29}$$

3 Numerical Solution Procedures

The problems as formulated in the preceding sections are state constrained optimal control problems. To solve these optimal control problems, it is necessary to use a numerical solution procedure which can determine the optimal admissible control functions $\alpha_S(t)$ and $\alpha_T(t)$ with corresponding response $\eta(x,t)$, $u(x,t)$ and $\mu(x,t)$, $\lambda(x,t)$ satisfying the flow and the associated adjoint equations. The procedure which is developed for this purpose consists of a constrained optimisation algorithm for iteratively determining the optimal control functions, together with a finite difference scheme for solving the flow and adjoint equations.

3.1 Optimisation Algorithms

It is well established that if the functional gradients can be evaluated analytically, gradient based optimisation algorithms tend to have superior convergence properties as compared to those which do not use the gradient. Therefore two gradient based optimisation algorithms, which have been tested thoroughly in [1], are used in the current work. These are the conditional gradient algorithm (CGA) and the projected gradient algorithm (PGA). The structures of the two algorithms are illustrated in Fig.2 and Fig.3 respectively. Both algorithms employ a simple but efficient step length rule which halves the current step length if the current control functions fail to improve the functional value over the previous iteration. The iteration is terminated when the measure $M(\underline{\alpha}^K)$ is less than a given tolerance, where $M(\underline{\alpha})$ is given by

$$M(\underline{\alpha}) = \max_{\underline{\beta} \in \underline{U}} < \nabla E(\underline{\alpha}), \underline{\beta} - \underline{\alpha} > = < \nabla E(\underline{\alpha}), \underline{\tilde{\alpha}} - \underline{\alpha} > \tag{30}$$

and $\underline{U}$ is the set of admissible controls. In the conditional gradient algorithm $\underline{\tilde{\alpha}}$ is used as the search direction for the new control. In the projected gradient algorithm, however, it is used solely for calculating the first variation for the convergence criterion.

3.2 Finite Difference Scheme

It can be seen that both state and adjoint equations are partial differential equations of hyperbolic type. To solve these equations numerically, an explicit leapfrog finite difference scheme is used. The flow equations are integrated forward in time from an initial state (arbitrary) to obtain the final condition. This procedure is repeated, using the computed final condition as the new initial condition, until the periodic condition is satisfied. The adjoint equations are similarly integrated repeatedly backward in time from the final state. A non-staggered grid system is adopted. The grid arrangement and the relevant nomenclature for the finite difference scheme are shown in Fig.4.

For the tidal flow problem it is found that the advection term uu_x in the momentum equation (2) is negligible, and therefore in order to simplify the computation, the advection terms are not modelled numerically. With reference to Fig.4, the flow equations are discretised as follows

Continuity equation:

$$b_j^n \frac{\eta_j^{n+1} - \eta_j^{n-1}}{2\triangle t} + \frac{A_{j+1}^n u_{j+1}^n - A_{j-1}^n u_{j-1}^n}{2\triangle x} = 0 \tag{31}$$

The continuity equation is followed by a post processing step

$$\eta_j^n := (\eta_j^{n+1} + 2\eta_j^n + \eta_j^{n-1})/4$$

Momentum equation:

$$u_j^{n+1} = \left[\frac{u_j^{n-1}}{d_j^{n-1}} - \frac{\triangle t}{\triangle x} g(\eta_{j+1}^n - \eta_{j-1}^n)\right] \frac{1}{d_j^n} \tag{32}$$

where

$$d_j^n = 1 + (gn^2 |u_j^n| \triangle t) \frac{1}{(r_j^n)^{4/3}}$$

$$n = 1, 2, ..., NT - 2, NT - 1$$

$$j = 2, 3, ..., m - 2, m + 2, ..., NX - 2, NX - 1$$

where NT is the total number of time steps, $\triangle t = T/NT$ is the time step, NX is the total number of spatial grid points and $\triangle x$ is the spatial step. Separate spatial step values are allowed in the outer estuary and in the estuary basin. j is the grid point number on the finite difference grid. All the quantities with superscript n are evaluated at $t = n\triangle t$. It can be seen that this scheme is a three-level time-differencing scheme and has second-order accuracy in both space and time. The equations are easily rearranged to give formulae for η_j^{n+1} and u_j^{n+1} in terms of the other quantities. The quantities at $n-1$ and n must be stored in order to compute those at $n+1$.

As the scheme is of explicit type, we cannot guarantee that it is unconditionally stable. The stability of the resulting discretisation equations can be analysed by the Von Neuman method. For the explicit scheme, the stability criterion takes the form

$$CFL = \frac{c\triangle t}{\triangle x} \leq 1 \tag{33}$$

This is the Courant-Friedrichs-Lewy condition; CFL is the well-known Courant or CFL number, and $c(x) = g\sqrt{A(\eta, x)/b(\eta, x)}$ represents the local wave speed.

The boundary conditions for the flow equations are treated as follows:

Left Boundary (j=1)

$$\eta_1^{n+1} = f(t^{n+1}) \tag{34}$$

$$u_1^{n+1} = \left[\frac{u_1^{n-1}}{d_1^{n-1}} - \frac{\Delta t}{\Delta x_1} 2g(\eta_2^n - f(t^n))\right] \frac{1}{d_1^n} \tag{35}$$

Internal Boundary - Barrage (j=m $\pm$ 1)

$$b_{m-1}^n \frac{\eta_{m-1}^{n+1} - \eta_{m-1}^{n-1}}{2\Delta t} + \frac{qm - A_{m-2}^n u_{m-2}^n}{2\Delta x_1} = 0 \tag{36}$$

$$b_{m+1}^n \frac{\eta_{m+1}^{n+1} - \eta_{m+1}^{n-1}}{2\Delta t} + \frac{A_{m+2}^n u_{m+2}^n - qm}{2\Delta x_2} = 0 \tag{37}$$

where qm is the total volumetric flow rate of water across the barrage. From equation (6) we have

$$qm = \alpha_S(t^n) X_S(h^n) + \alpha_T(t^n) X_T(h^n)$$

and

$$h^n = \frac{1}{2}\left(\eta_{m-1}^{n+1} + \eta_{m-1}^{n-1} - \eta_{m+1}^{n+1} - \eta_{m+1}^{n-1}\right)$$

It is obvious that the above equations constitute a system of non-linear algebraic equations with two unknowns η_{m-1}^{n+1} and η_{m+1}^{n+1} and must be solved iteratively. A damped Newton method is used here. This method is known to have good convergence properties. Details can be found elsewhere.

After η_{m-1}^{n+1} and η_{m+1}^{n+1} are evaluated, the flows are determined from

$$u_{m-1}^{n+1} = \left[\frac{u_{m-1}^{n-1}}{d_{m-1}^{n-1}} - \frac{\Delta t}{\Delta x_1} g\left(\frac{1}{2}(\eta_{m-1}^{n+1} + \eta_{m-1}^{n-1}) - \eta_{m-2}^n\right)\right] \frac{1}{d_{m-1}^n} \tag{38}$$

$$u_{m+1}^{n+1} = \left[\frac{u_{m+1}^{n-1}}{d_{m+1}^{n-1}} - \frac{\Delta t}{\Delta x_2} g\left(\eta_{m+2}^n - \frac{1}{2}(\eta_{m+1}^{n+1} + \eta_{m+1}^{n-1})\right)\right] \frac{1}{d_{m+1}^n} \tag{39}$$

Right Boundary (j=NX)

$$u_{NX}^{n+1} = 0 \tag{40}$$

$$b_{NX}^{n}\frac{\eta_{NX}^{n+1} - \eta_{NX}^{n-1}}{2\triangle t} - \frac{2A_{NX-1}^{n}u_{NX-1}^{n}}{2\triangle x_2} = 0 \tag{41}$$

Similarly the finite difference forms of the adjoint equations are written as

Adjoint continuity equation:

$$b_j^n\left(\frac{\lambda_j^{n-1} - \lambda_j^{n+1}}{2\triangle t} - u_j^n\frac{\lambda_{j+1}^n - \lambda_{j-1}^n}{2\triangle x}\right) - g\frac{\mu_{j+1}^n - \mu_{j-1}^n}{2\triangle x} - \mu_j^n\frac{4gn^2|u_j^n|u_j^n(r')_j^n}{3(r_j^n)^{7/3}} = 0 \tag{42}$$

Again the adjoint continuity equation is followed by a post-processing step

$$\lambda_j^n := (\lambda_j^{n+1} + 2\lambda_j^n + \lambda_j^{n-1})/4$$

Adjoint momentum equation:

$$\mu_j^{n-1} = \left[\mu_j^{n+1}(1 - q_j^n) + \frac{\triangle t}{\triangle x}(\lambda_{j+1}^n - \lambda_{j-1}^n)A_j^n\right]\frac{1}{1 + q_j^n} \tag{43}$$

where

$$q_j^n = 2\triangle t g n^2|u_j^n|\frac{1}{(r_j^n)^{4/3}}$$

$$n = NT, NT - 1, ..., 1$$

$$j = 2, 3, ..., m - 2, m + 2, ..., NX - 2, NX - 1$$

The boundary conditions for the adjoint equations are treated as follows:

Left Boundary (j=1)

$$\mu_1^{n-1} = \left[\mu_1^{n+1}(1 - q_1^n) + 2\frac{\triangle t}{\triangle x_1}\lambda_2^n A_1^n\right]\frac{1}{1 + q_1^n} \tag{44}$$

$$\lambda_1^{n-1} = 0 \tag{45}$$

Internal Boundary - Barrage (j=m $\pm$ 1)

$$b^n_{m-1}\frac{\lambda^{n+1}_{m-1}-\lambda^{n-1}_{m-1}}{2\Delta t}+b^n_{m-1}u^n_{m-1}\left[\frac{(\lambda^{n-1}_{m-1}+\lambda^{n+1}_{m-1})/2-\lambda^n_{m-2}}{2\Delta x_1}\right]+$$

$$g\frac{mm-\mu^n_{m-2}}{2\Delta x_1}+\mu^n_{m-1}\beta_{m-1}=0 \qquad (46)$$

$$b^n_{m+1}\frac{\lambda^{n+1}_{m+1}-\lambda^{n-1}_{m+1}}{2\Delta t}+b^n_{m+1}u^n_{m+1}\left[\frac{\lambda^n_{m+2}-(\lambda^{n-1}_{m+1}+\lambda^{n+1}_{m+1})/2}{2\Delta x_2}\right]+$$

$$g\frac{\mu^n_{m+2}-mp}{2\Delta x_2}+\mu^n_{m+1}\beta_{m+1}=0 \qquad (47)$$

where

$$\beta_{m\pm1}=\frac{4gn^2u^n_{m\pm1}|u^n_{m\pm1}|(r')^n_{m\pm1}}{3(r^n_{m\pm1})^{7/3}}=0$$

$$g\cdot mp+\gamma^n(\alpha_S(t^n)X_S(h^n)'+\alpha_T(t^n)X_T(h^n)')=\left(\frac{\partial e}{\partial h}\right)^n$$

$$\gamma^n = \frac{1}{2}(\lambda^{n-1}_{m-1}+\lambda^{n+1}_{m-1}-\lambda^{n-1}_{m+1}-\lambda^{n-1}_{m+1})$$

$$mm = mp$$

These equations give a pair of linear equations for λ^{n-1}_{m+1}, λ^{n-1}_{m-1} which are solved directly. The adjoint flows are then found from

$$\mu^{n-1}_{m-1}=\left[\mu^{n+1}_{m-1}(1-q^n_{m-1})+\frac{\Delta t}{\Delta x_1}\left(\frac{1}{2}(\lambda^{n+1}_{m-1}+\lambda^{n-1}_{m-1})-\lambda^n_{m-2}\right)A^n_{m-1}\right]\frac{1}{1+q^n_{m-1}} \qquad (48)$$

$$\mu^{n-1}_{m+1}=\left[\mu^{n+1}_{m+1}(1-q^n_{m+1})+\frac{\Delta t}{\Delta x_2}\left(\lambda^n_{m+2}-\frac{1}{2}(\lambda^{n+1}_{m+1}+\lambda^{n-1}_{m+1})\right)A^n_{m+1}\right]\frac{1}{1+q^n_{m+1}} \qquad (49)$$

Right Boundary (j=NX)

$$\mu^{n-1}_{NX}=0 \qquad (50)$$

$$b^n_{NX}\frac{\lambda^{n-1}_{NX}-\lambda^{n+1}_{NX}}{2\Delta t}+g\frac{2\mu^n_{NX-1}}{2\Delta x_2}=0 \qquad (51)$$

4 Results and Discussion

In order to examine and compare the performance of the two optimisation algorithms, numerical results are obtained for a practical problem which simulates the proposed Severn estuary tidal barrage scheme in 1981 [7]. The model extends 120 km from Ilfracombe to Sharpness and the barrage is assumed to contain 140 turbines and 160 sluices. Discharge and derived power characteristics are the same as those for the early study and, essentially follow the line of maximum efficiency until the maximum power limitation is reached [5]. The data and functions necessary for the computation, such as tidal elevation and turbine flow characteristics, are prescribed as follows:

1) Turbine flow functions

$$Q_{T1} = 140 \times 390.0(1 - tanh(10(h + 2.27))$$

$$Q_{T2} = \begin{cases} 140 \times 390.0(1 + tanh(10(h - 2.27)) & \text{for two-way scheme} \\ 140 \times 102.9048\sqrt{2gh} & \text{for ebb scheme} \end{cases}$$

2) Sluice flow functions

$$Q_{S1} = 160 \times 259.2\sqrt{-2gh}$$

$$Q_{S2} = 160 \times 259.2\sqrt{2gh}$$

3) Tidal elevation $f(t)$:

$$f(t) = F_o cos(\frac{2\pi t}{T}) + 0.15$$

where F_o is the tidal amplitude in metres and for this problem is 4.25.

4) Power function e:

$$e = C(t)\alpha_T(t)F(h)$$

where C is the tariff and $F(h)$ is the turbine power characteristic. Here C takes a constant value of 2.43 and $F(h)$ takes the following form

$$F(h) = \begin{cases} 0 & \text{if } |h| < 2.27 \\ 0.039671|h|^3 - 0.91158|h|^2 + 14.113|h| - 23.79 & \text{if } 2.27 \leq |h| \leq 8.82 \\ 57.0 & \text{if } |h| > 8.82 \end{cases}$$

This power characteristic should be valid for an ebb scheme as well as for a two-way scheme. However in an ebb scheme, there is no instantaneous power output when the head difference is positive and therefore the power characteristics should be set to zero. It should be noted that the unit of the power function is megawatts.

5) Manning's number = 0.04

6) Estuarine breadth $b(\eta, x)$ and area $A(\eta, x)$: These are numerically approximated by taking a linear interpolation between the low water breadths and high water breadths (see Fig.5 and Fig.6).

The test data are chosen to enable comparisons to be made with previous results [5]. In practice the functions X_T, X_S should be defined such that $X_T = 0, X_S = 0$ only when $h = 0$. In the present case, where this does not hold, the optimal control α_T is undefined in regions where both e and X_T are zero, and α_T takes arbitrary values in these regions. The optimality of the solution is not afffected, however, as the power generated depends only on the *actual* flow through turbines and sluices. A more suitable choice for X_T in this model is obtained by defining X_T for $|h| < 2.27$ to be equal to the maximum flow through the turbines used as sluices. Such a choice gives similar results to those presented here.

Both two-way and ebb schemes are computed for a half day cycle with a tidal period 12.4 hours (14,714 seconds). The computation uses 250 time steps for both flow and adjoint equations. With regard to the spatial discretisation, the outer estuary is discretised with a total of 15 mesh points whereas the estuary basin is discretised with 11 mesh points. As it is known that the length of the outer estuary and the estuary basin is 70.0 km and 50.0 km respectively; this results in an equally distributed spatial step of 5.0 km throughout the whole estuary. Based on the above chosen time and spatial steps, the CFL numbers can be evaluated. It is found that the maximum CFL number is 0.6987. Therefore the Courant condition is satisfied and the finite difference scheme is stable.

Two sets of initial controls are used. These are: 1) $\alpha_S^o = 0.1$, $\alpha_T^o = 1.0$ and 2) $\alpha_S^o = \frac{1+sgn(f(t))}{2}$, $\alpha_T^o = \frac{1-sgn(f(t))}{2}$. The second set of initial controls simulates an ebb scheme. Detailed computational results using CGA and PGA are tabulated in Table 1 for the ebb only scheme and Table 2 for the two-way generation scheme respectively. These results are also presented in graphical form in Figs.7-14. It should be mentioned that throughout the investigation the convergence tolerance employed is 1.5% of the power functional.

An examination of the results shows that in general the two algorithms perform quite well, considering the fact that the test data used are pretty rough. For a majority of the test runs convergence is achieved within 10 iterations. As far as rate of convergence is concerned, it is observed that for the ebb scheme the conditional gradient algorithm appears to perform better, whereas for the two-way scheme the projected gradient algorithm does. This observation differs from the previous work using the flat basin flow model where, with a linear power function, the conditional gradient algorithm proved to have better convergence properties for two-way schemes as well as ebb schemes. However, with the current system it can not be established theoretically for a linear power function that the optimal control functions are strictly bang-bang in nature, and in practice the optimal turbine control strategy is found to contain interior values even in the linear case.

It is further observed from Tables 1 and 2 that in terms of power output the ebb schemes are superior to the two-way schemes in all cases investigated. In the ebb schemes the power outputs predicted by the two algorithms are in agreement to within 1.0%. The algorithms are able to predict that the turbines are used for sluicing when they are not generating. This is indicated in the graphs by intervals where positive turbine flow is shown but energy is not produced.

In the two-way schemes, by contrast, there are some discrepancies in the predicted power outputs with different sets of initial controls, as shown in Table 2. Similar results are also reported by Birkett [6] who made an investigation of a modified conditional gradient algorithm for non-linear optimal control problems using the flat basin model. He concluded that the control strategy computed by the algorithm for the two-way scheme is only a local maximum. That seems to be the case with the current results. In fact, if the second set of initial controls is used, the optimised two-way schemes produce a power output as well as an optimal control strategy close to that of the ebb scheme. It is worth pointing out that even though the ebb schemes produce more power than the corresponding two-way schemes, it doesn't necessarily mean that we should not consider the two-way scheme in practice. In certain circumstances it may be more important to be able to supply electricity flexibly over a wide time period.

5 Conclusions

In this report we further investigate non-linear optimal control problems for a tidal power scheme. A sophisticated dynamic flow model is used for accurate description of the fluid dynamics in the estuary and across the barrage. By using the Lagrangian method the necessary conditions for optimality are established.

Two gradient based iterative optimisation algorithms are used to solve the optimal control problems numerically. Computational results are obtained for a practical problem which simulates the proposed Severn estuary tidal barrage scheme. Generally speaking, the algorithms perform well, requiring only a few iterations. The finite difference methods for the numerical solution of the flow and adjoint equations are accurate and stable. It is found from the computation that an ebb scheme is superior to a two-way scheme in all cases investigated.

Finally it can be concluded that the optimal control approach to the tidal power generation problem is a feasible and attractive method for systematically computing flow control strategies.

Acknowledgements

The research reported here has been conducted with financial support from National Power (NPTec) and this support is gratefully acknowledged.

References

[1] Xu, Z.G. and Nichols, N.K., "An Investigation of the Form of an Optimal Controller in a Tidal Power Generation Scheme with Two Controls", Numerical Analysis Report NA.5/91, Department of Mathematics, University of Reading, 1991.

[2] Andrews, T.P., Nichols, N.K. and Xu, Z.G. "The Form of Optimal Controllers for Tidal Power Generation Schemes", Numerical Analysis Report NA.8/90, Department of Mathematics, University of Reading, 1990.

[3] Pontryagin, L.S., Boltyanskii, V.G. and Gamkrelidze, R.V., " The Mathematical Theory of Optimal Processes", Interscience, 1962.

[4] Birkett, N.R.C. and Nichols, N.K., "Optimal Control Problems in Tidal Power Generation", Numerical Analysis Report NA.8/83, Department of Mathematics, University of Reading, 1983.

[5] Birkett, N.R.C., "Nonlinear Optimal Control of Tidal Power Schemes in Long Estuaries", Numerical Analysis Report NA.9/86, Department of Mathematics, University of Reading, 1986.

[6] Birkett, N.R.C., "Nonlinear Optimal Control Problems in Tidal Power Calculations", Numerical Analysis Report NA.2/85, Department of Mathematics, University of Reading, 1985.

[7] H.M.S.O., "Tidal Power from the Severn Estuary", Energy Paper No.46, 1981.

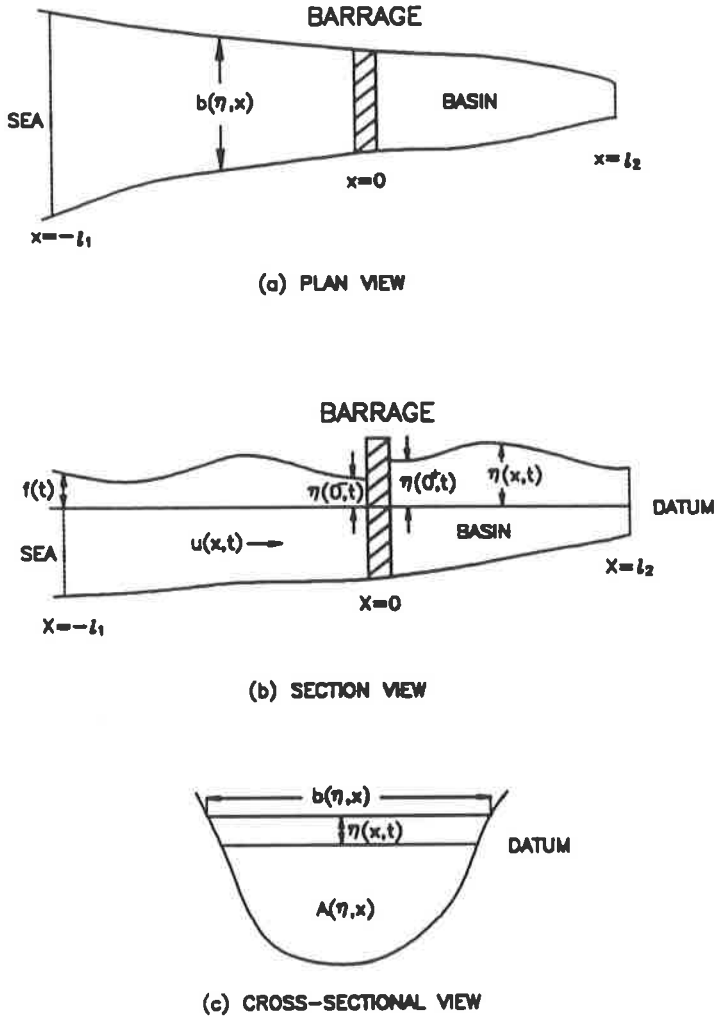

Figure 1: Estuary Geometry

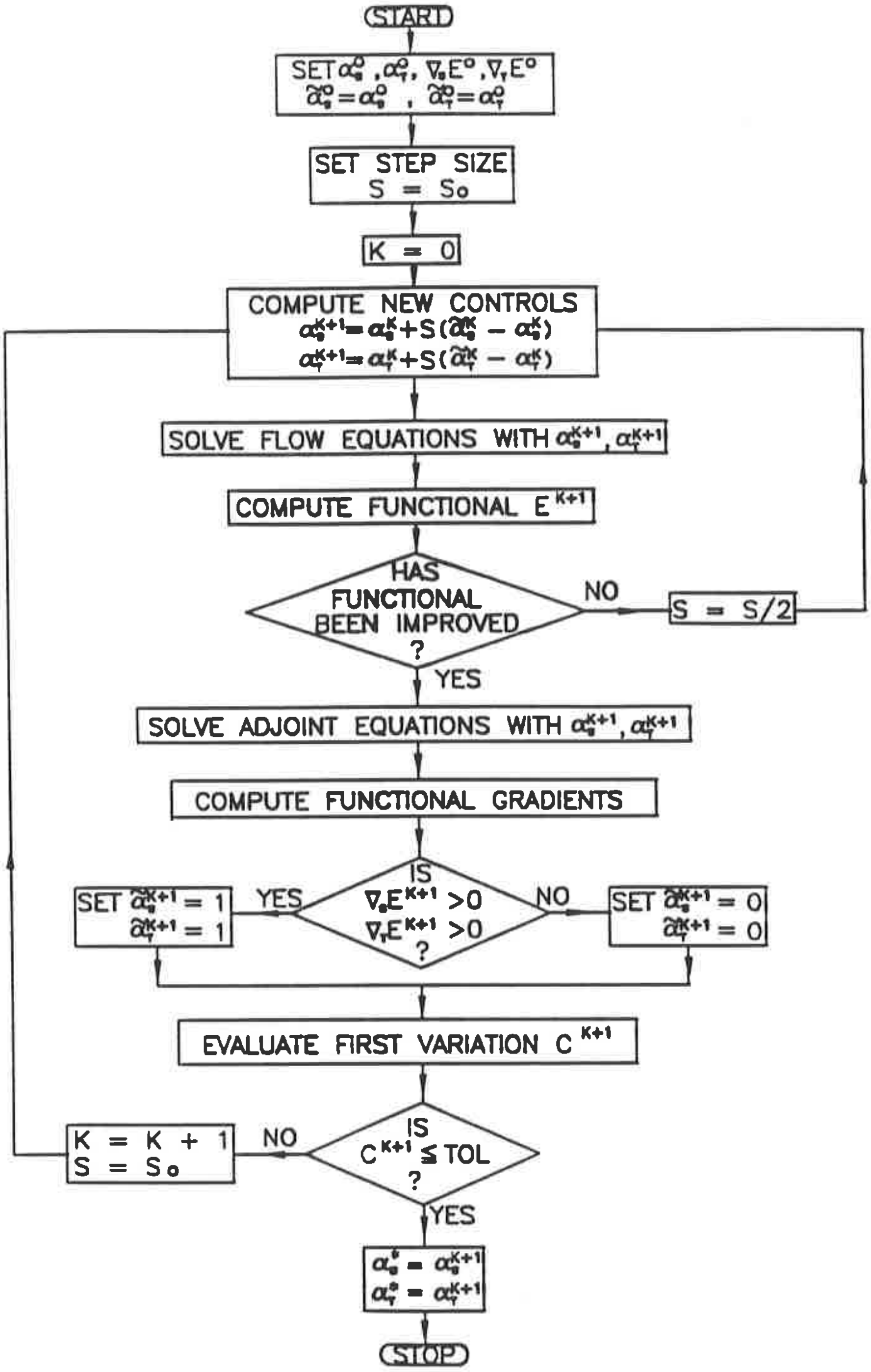

Figure 2: Flow chart - Conditional gradient algorithm (CGA)

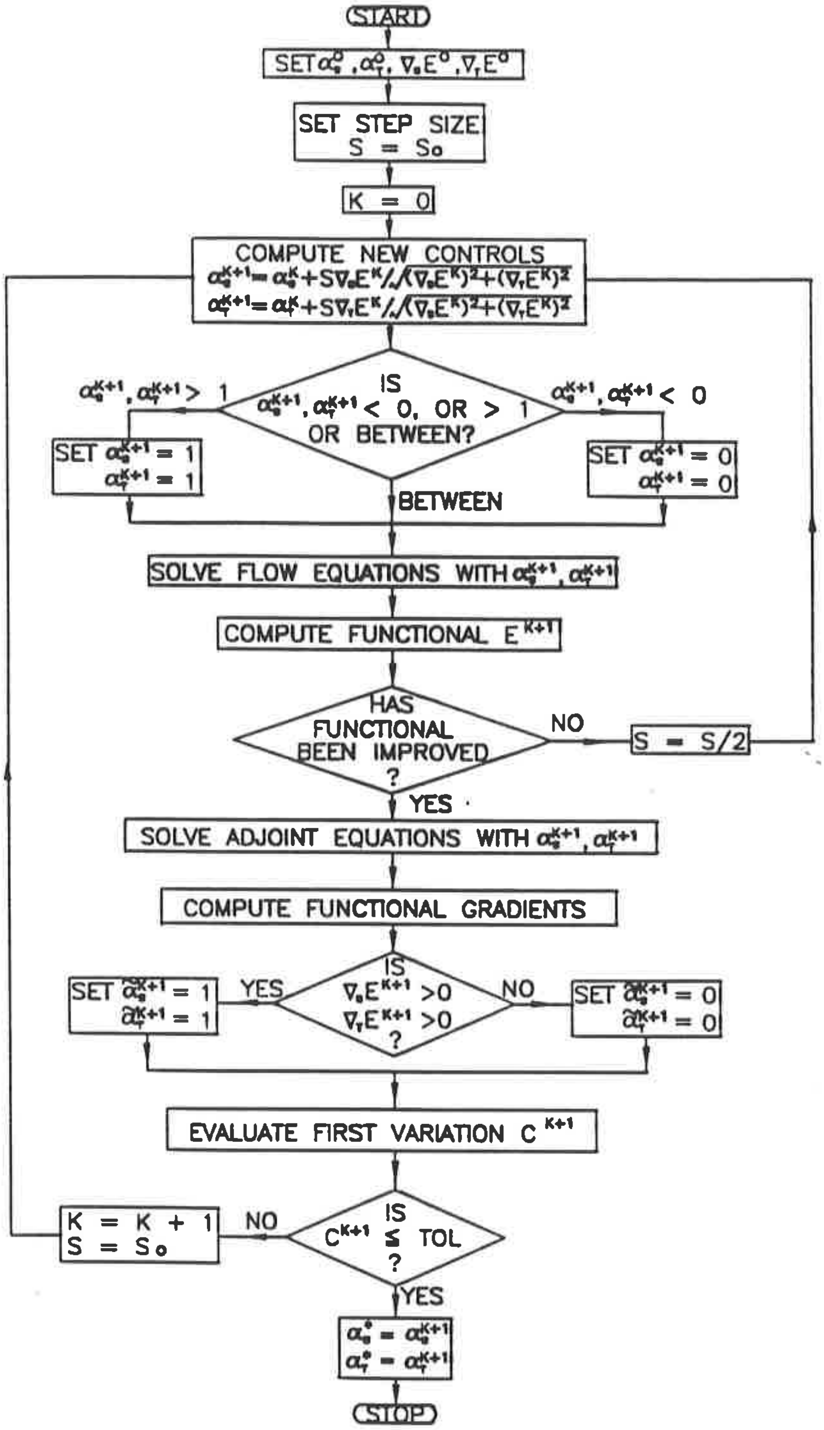

Figure 3: Flow chart - Projected gradient algorithm (PGA)

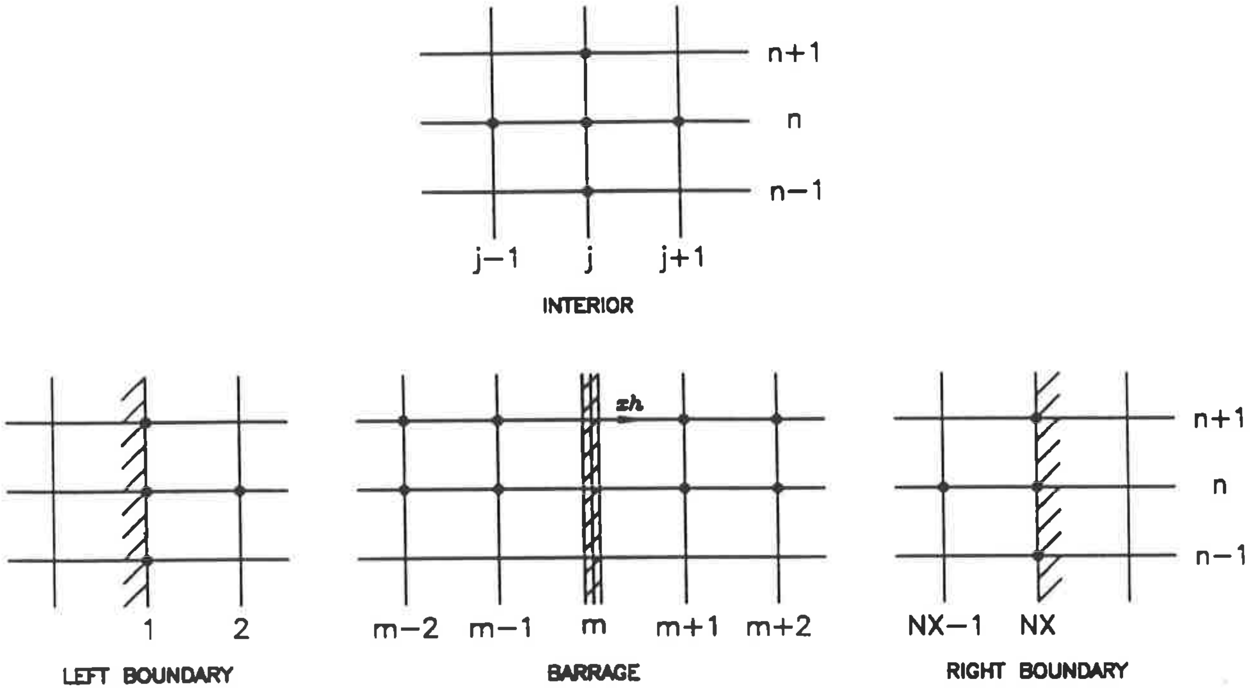

Figure 4: Finite Difference Grid

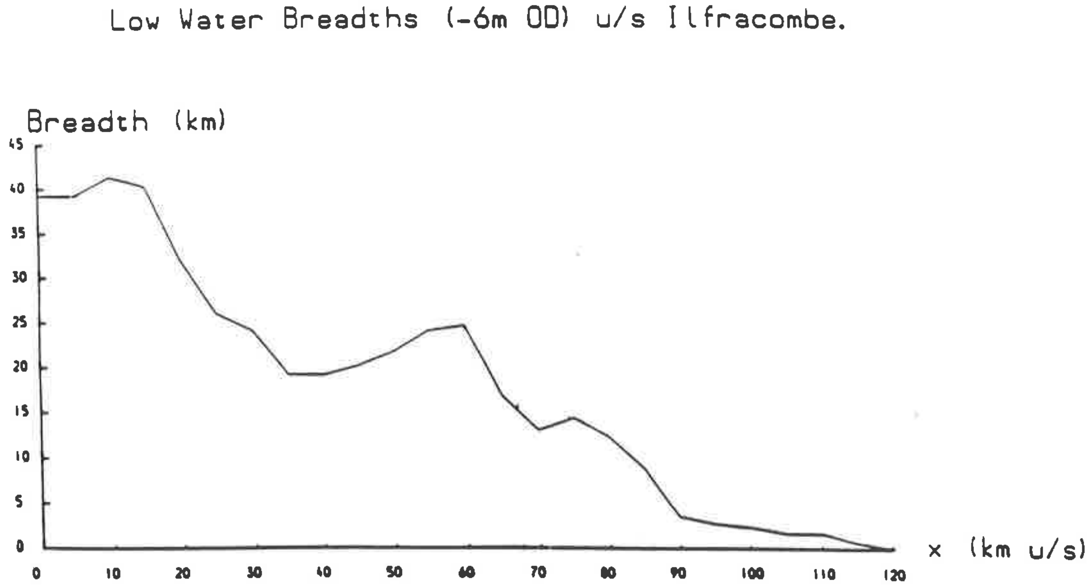

Figure 5: Low Water Breadths

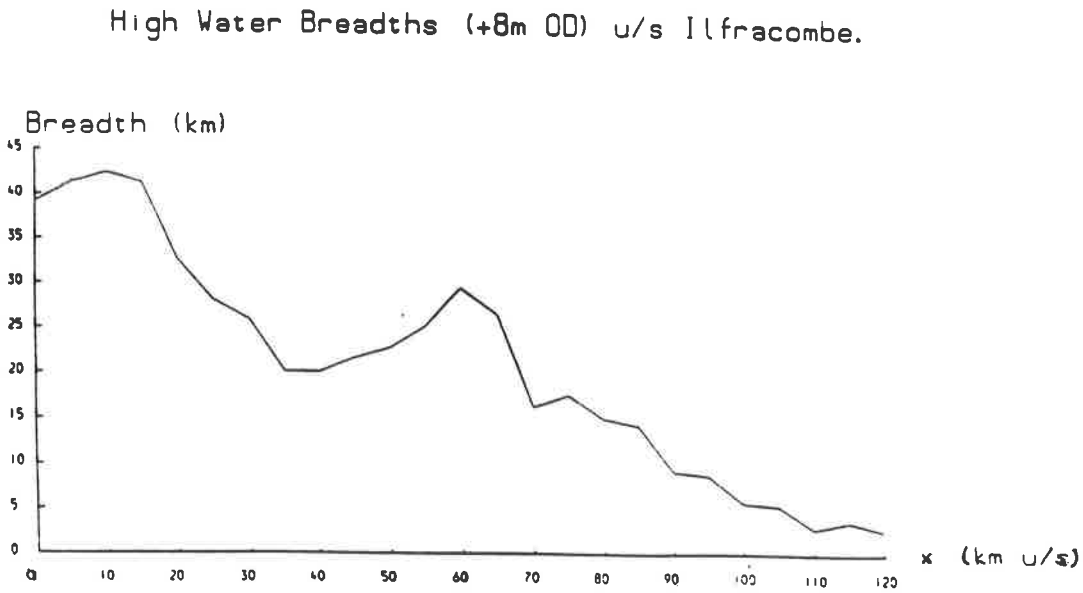

Figure 6: High Water Breadths

Table 1. EBB SCHEME

$\overset{\circ}{\alpha}_S$	$\overset{\circ}{\alpha}_T$	Power Output (GW)		No. of Iterations	
		CGA	PGA	CGA	PGA
0.1	1.0	4.93501	4.88295	8(11)	10(11)
(1+isgn(f(t)))/2	(1−isgn(f(t)))/2	4.91537	4.90474	9(11)	9(12)

Table 2. TWO–WAY SCHEME

$\overset{\circ}{\alpha}_S$	$\overset{\circ}{\alpha}_T$	Power Output (GW)		No. of Iterations	
		CGA	PGA	CGA	PGA
0.1	1.0	4.15528	4.38866	15(24)	8(8)
(1+isgn(f(t)))/2	(1−isgn(f(t)))/2	4.66008	4.67056	10(12)	8(8)

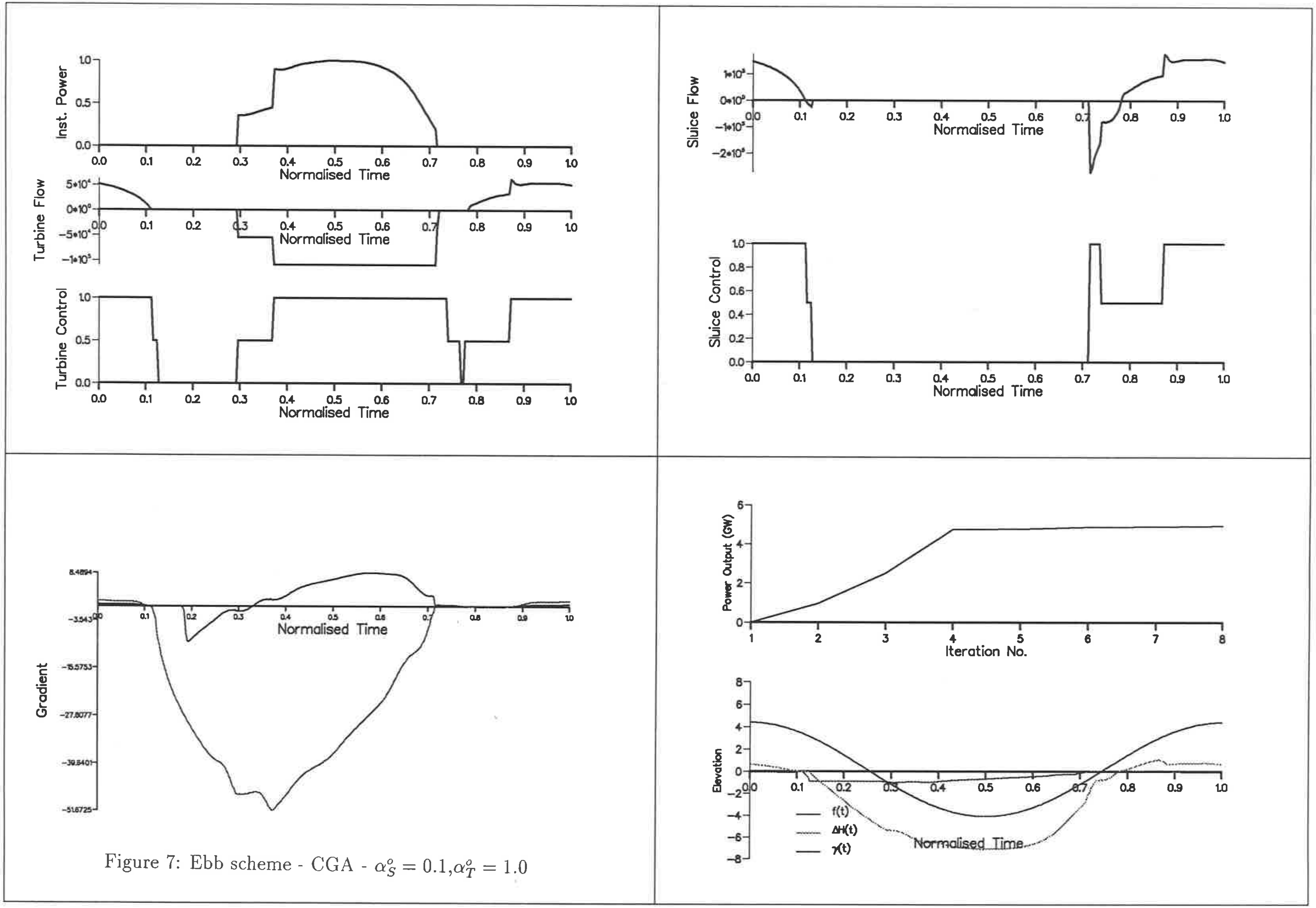

Figure 7: Ebb scheme - CGA - $\alpha_S^o = 0.1, \alpha_T^o = 1.0$

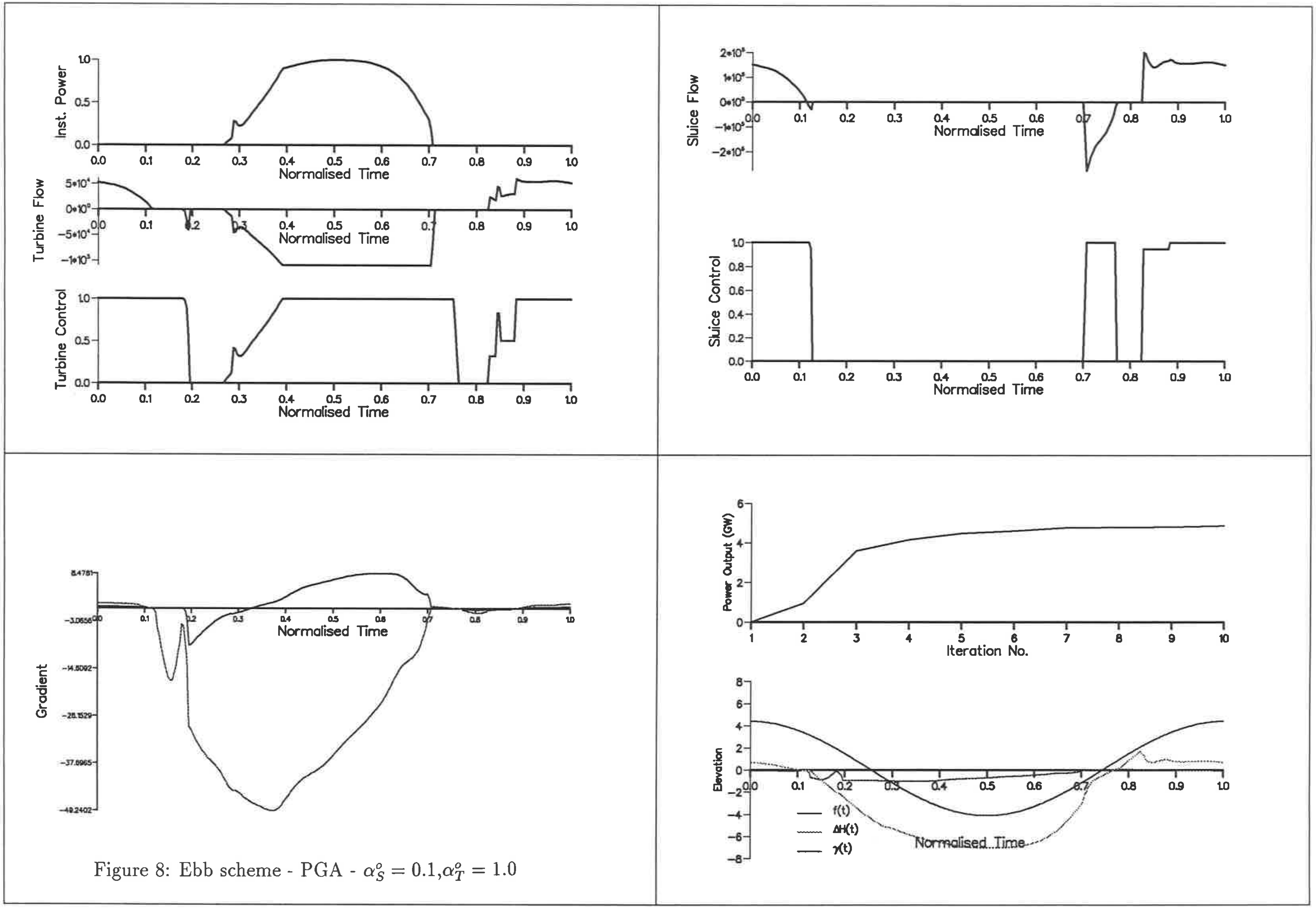

Figure 8: Ebb scheme - PGA - $\alpha_S^o = 0.1, \alpha_T^o = 1.0$

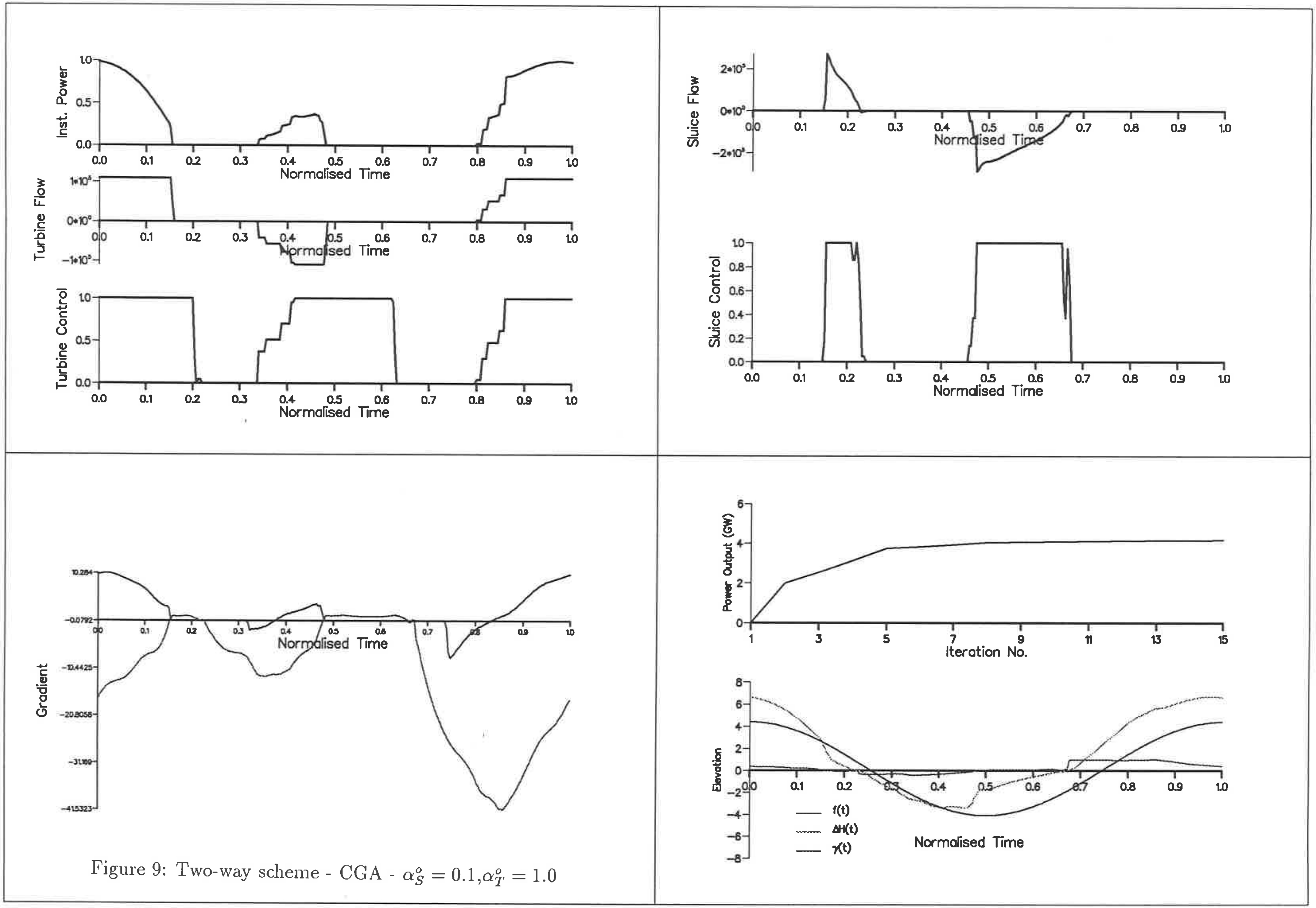

Figure 9: Two-way scheme - CGA - $\alpha_S^o = 0.1, \alpha_T^o = 1.0$

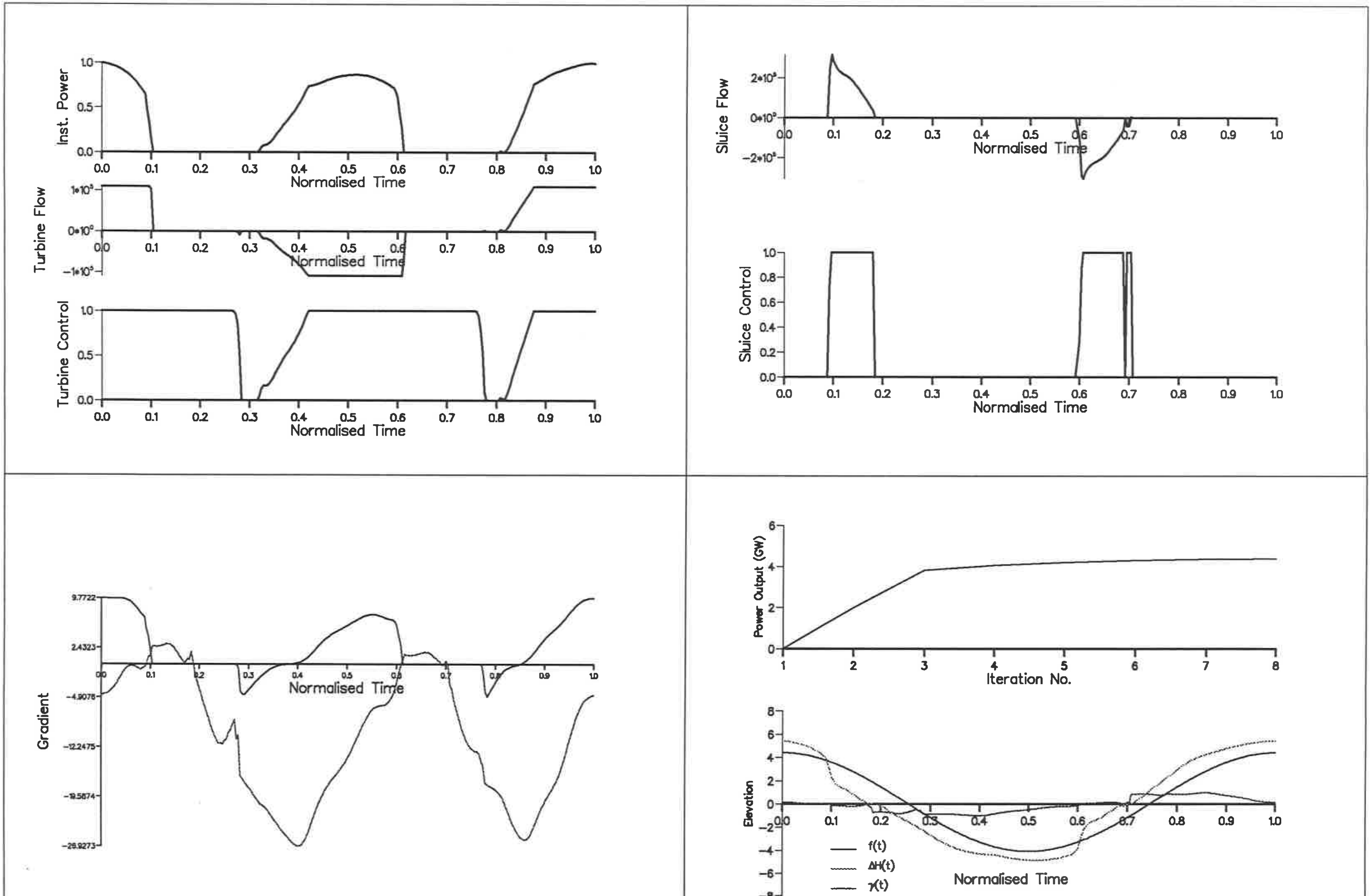

Figure 10: Two-way scheme - PGA - $\alpha_S^o = 0.1, \alpha_T^o = 1.0$

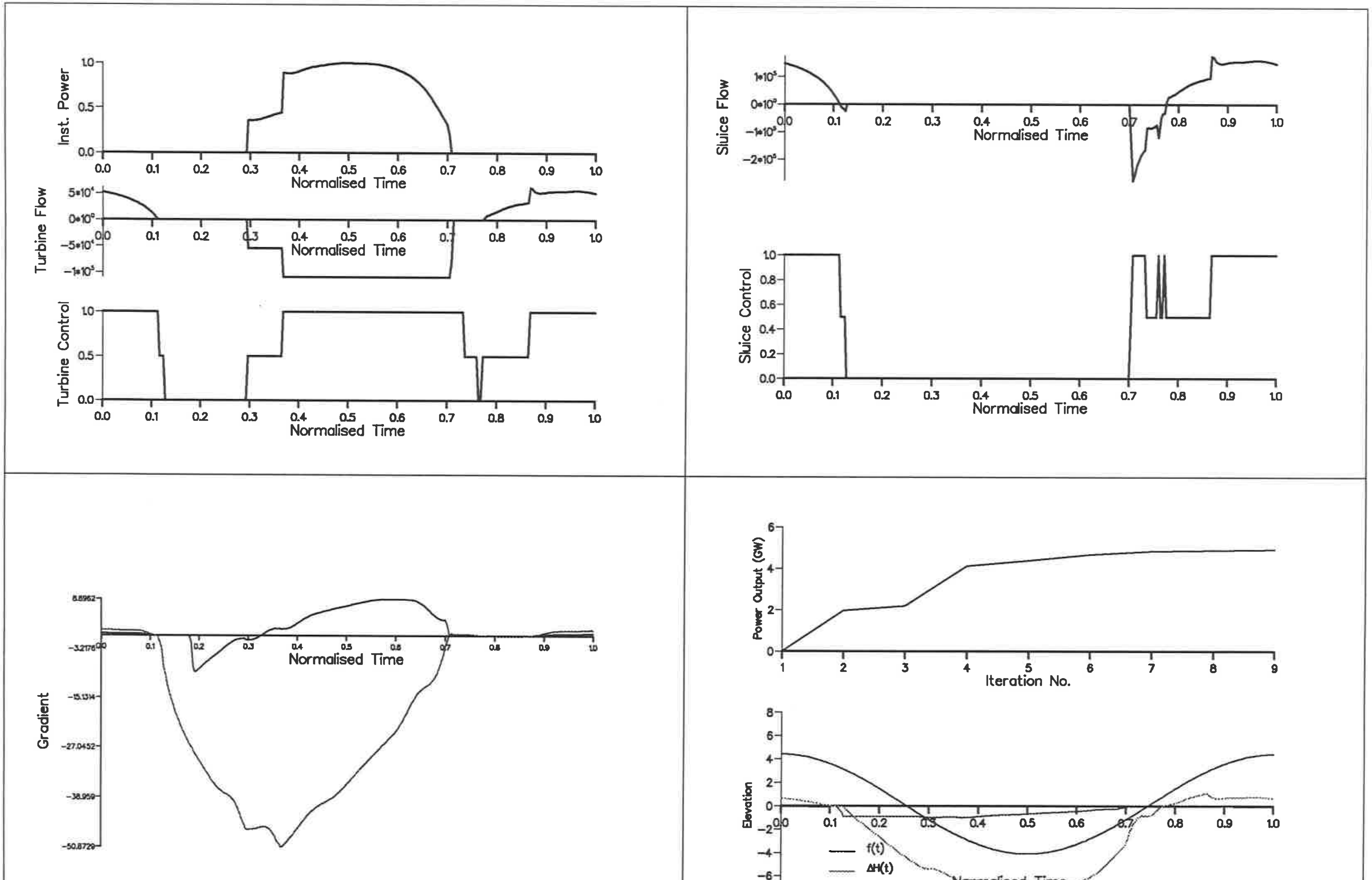

Figure 11: Ebb scheme - CGA - $\alpha_S^o = \frac{1+sgn(f)}{2}$, $\alpha_T^o = \frac{1-sgn(f)}{2}$

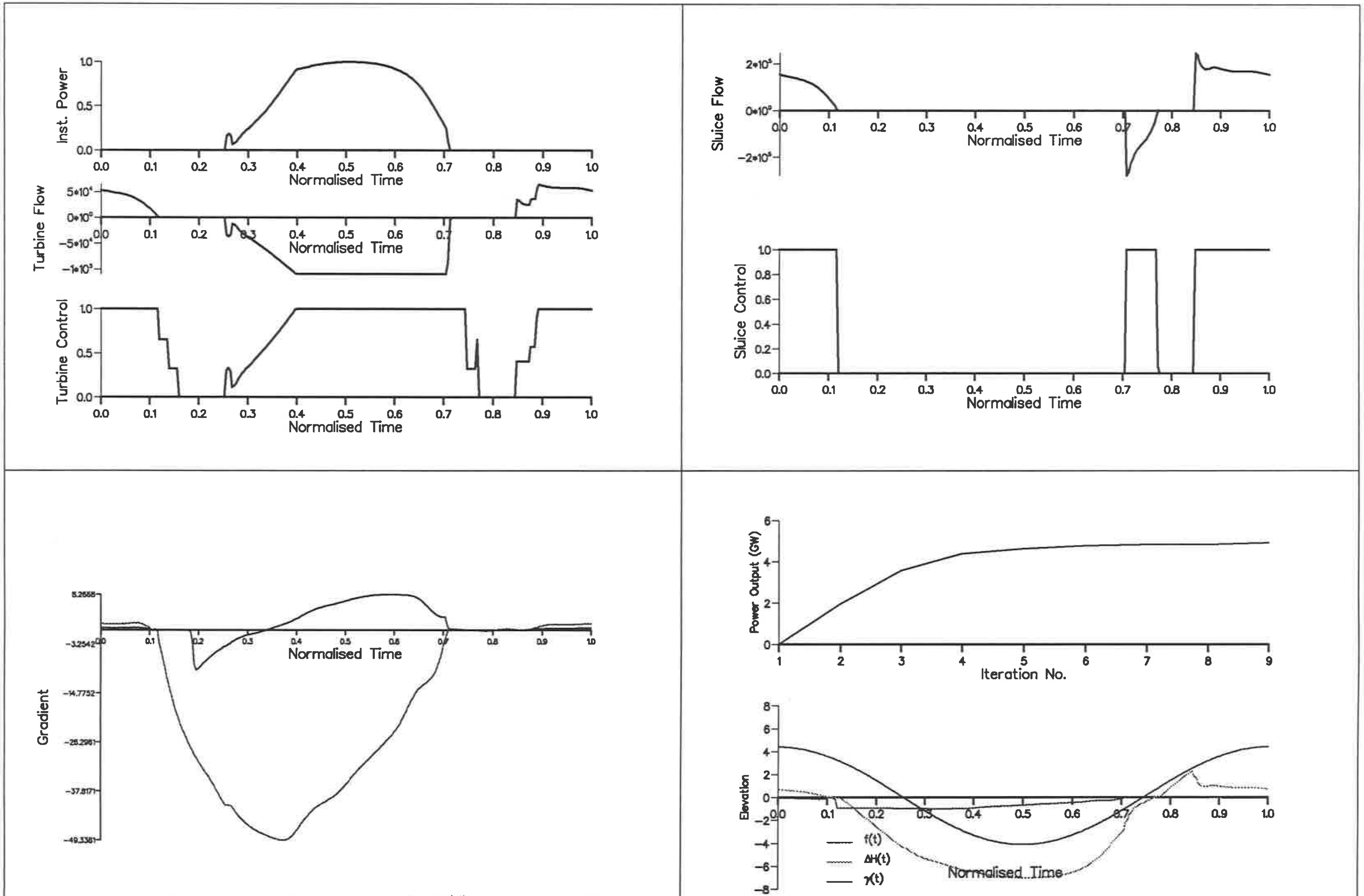

Figure 12: Ebb scheme - PGA - $\alpha_S^o = \frac{1+sgn(f)}{2}$, $\alpha_T^o = \frac{1-sgn(f)}{2}$

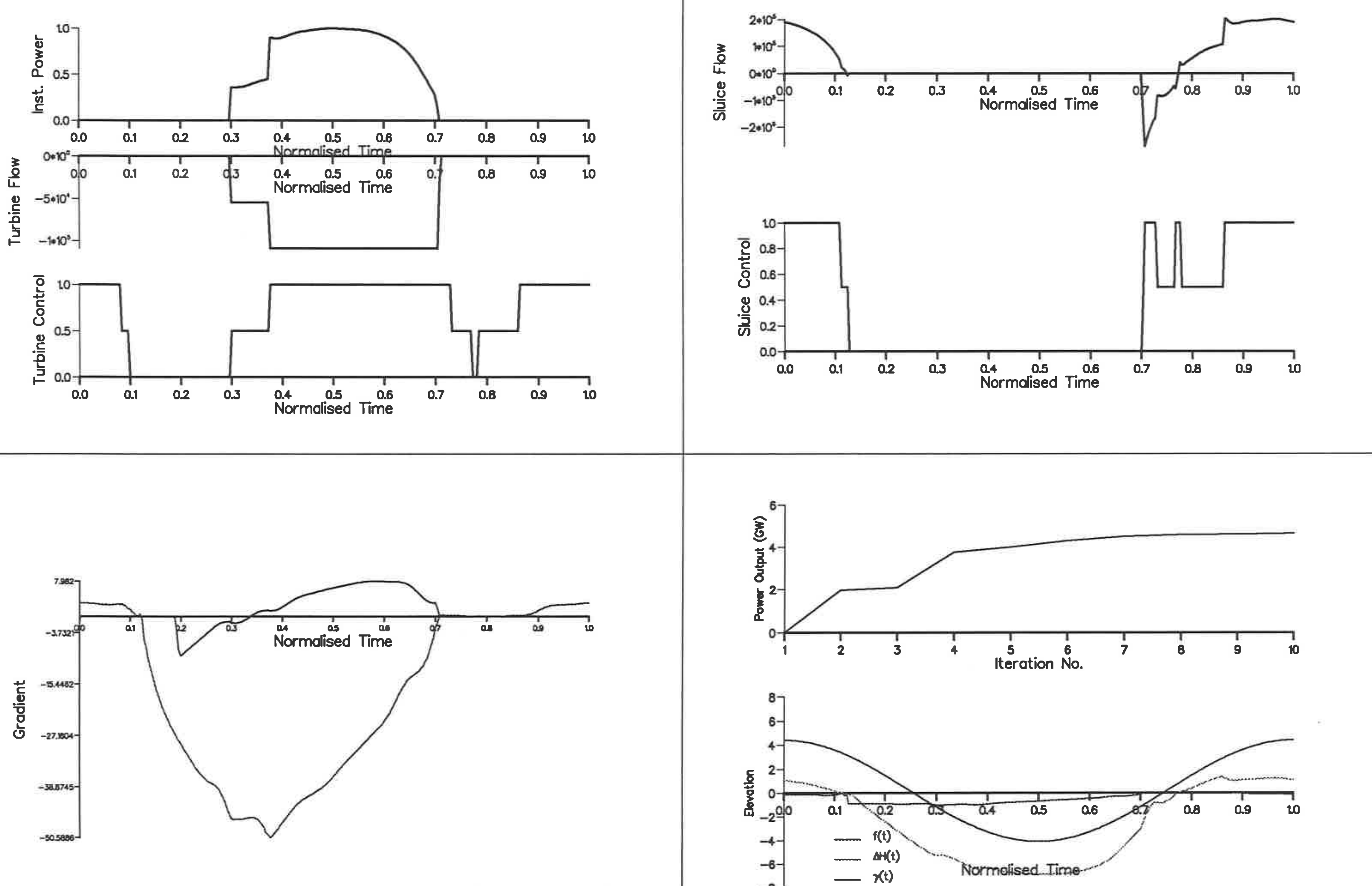

Figure 13: Two-way scheme - CGA - $\alpha_S^o = \frac{1+sgn(f)}{2}$, $\alpha_T^o = \frac{1-sgn(f)}{2}$

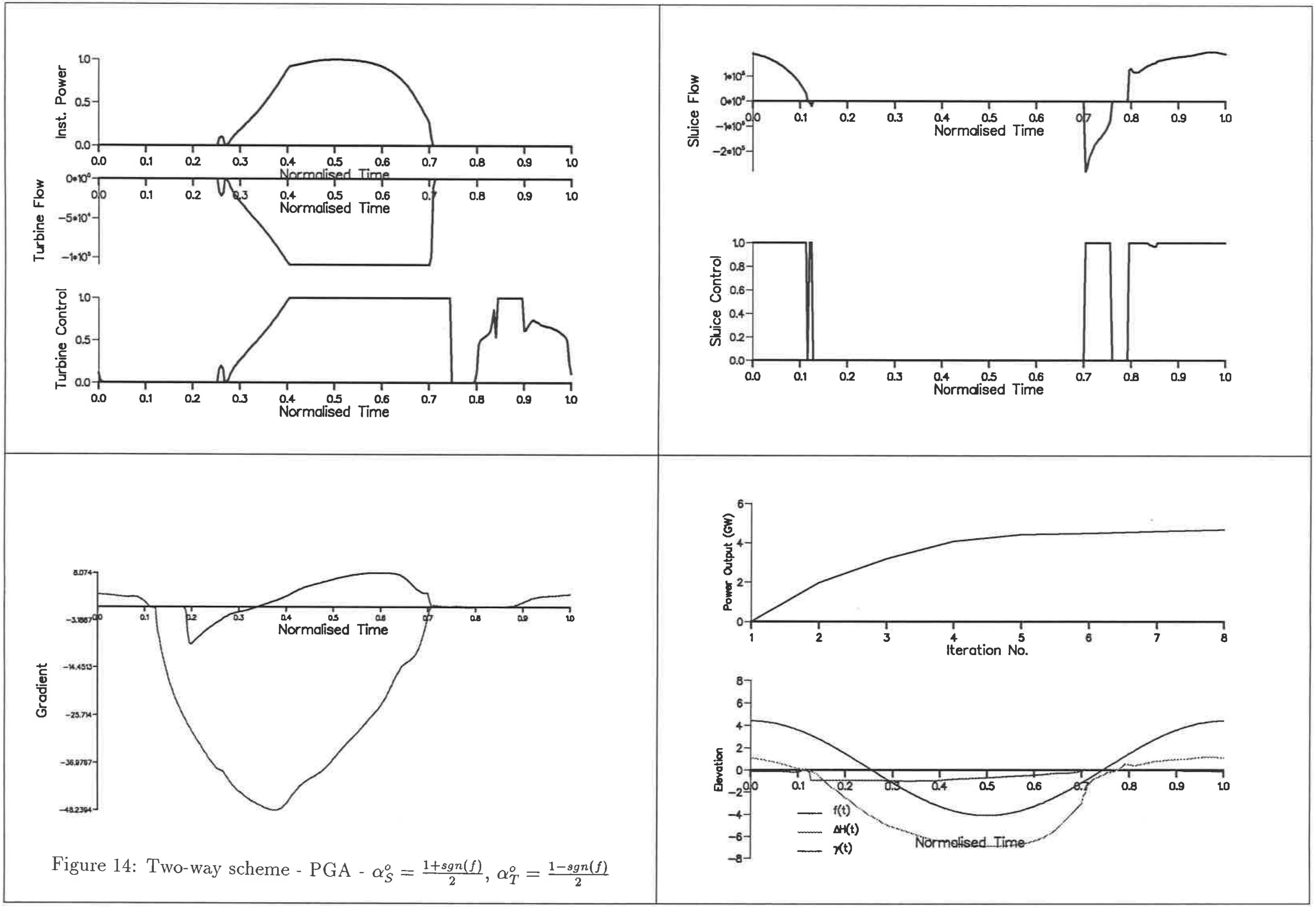

Figure 14: Two-way scheme - PGA - $\alpha_S^o = \frac{1+sgn(f)}{2}$, $\alpha_T^o = \frac{1-sgn(f)}{2}$